Blind source separation to enhance spectral and non-linear features of magnetoencephalogram recordings

Blind source separation to enhance spectral and non-linear features of magnetoencephalogram recordings. Application to Alzheimer's disease

Javier Escudero[1], Roberto Hornero[1], Daniel Abásolo[1], Alberto Fernández[2]

[1]Biomedical Engineering Group, E.T.S. Ingenieros de Telecomunicación, University of Valladolid, Spain

[2]Centro de Magnetoencefalografía Dr. Pérez-Modrego, Complutense University of Madrid, Spain

AUTHOR'S ADDRESS: Javier Escudero

E.T.S. Ingenieros de Telecomunicación

University of Valladolid

Camino del Cementerio s/n

47011 – Valladolid (Spain)

E-mail: javier.escudero@ieee.org

Abstract

This work studied whether a blind source separation (BSS) and component selection procedure could increase the differences between Alzheimer's disease (AD) patients and control subjects' spectral and non-linear features of magnetoencephalogram (MEG) recordings. MEGs were acquired with a 148-channel whole-head magnetometer from 62 subjects (36 AD patients and 26 controls), who were divided randomly into training and test sets. MEGs were decomposed using the algorithm for multiple unknown signals extraction (AMUSE). The extracted AMUSE components were characterised with two spectral – median frequency and spectral entropy (*SpecEn*) – and two non-linear features: Lempel-Ziv complexity (*LZC*) and sample entropy (*SampEn*). One-way analyses of variance with age as a covariate were applied to the training set to decide which components had the most significant differences between groups. Then, partial reconstructions of the MEGs were computed with these significant components. In the test set, the accuracy and area under the ROC curve (AUC) associated with each partial reconstruction of the MEGs were compared with the case where no BSS-preprocessing was applied. This preprocessing increased the AUCs between 0.013 and 0.227, while the accuracy for *SpecEn*, *LZC* and *SampEn* rose between 6.4% and 22.6%, improving the separation between AD patients and control subjects.

Keywords: Algorithm for multiple unknown signal extraction (AMUSE); Alzheimer's disease (AD); blind source separation (BSS); magnetoencephalogram (MEG); non-linear analysis; spectral analysis.

1. Introduction

Magnetoencephalogram (MEG) signals reflect the brain magnetic fields non-invasively [1]. This recording is closely related to the commonly used electroencephalogram (EEG) [1]. Although MEG equipment is more complex and expensive than EEG systems, the acquisition of the brain magnetic fields has some advantages over the EEG. For example, MEG signals are independent of any reference point. Additionally, they are less affected by extracerebral tissues than the EEG [1]. Thus, MEG can be useful to explore both normal and abnormal brain activities [1], such as the alterations caused by Alzheimer's disease (AD).

AD is the most common neurodegenerative disorder among elderly people in western countries [2]. It causes a progressive and irreparable impairment of mental functions which leads to the patient's death [2,3]. Moreover, AD diagnosis largely depends on the exclusion of other dementias and it can only be confirmed by necropsy [2,3]. Due to the fact that AD affects the brain cortex and that the EEG and MEG reflect brain cortical activity, the usefulness of these recordings to help in the diagnosis of this dementia has been extensively researched in the last decades [3,4].

EEG and MEG have been analysed with several signal processing techniques to gain insight into AD [3–5]. For instance, spectral features have been used to quantify the abnormalities in the spectra of AD patients' EEGs and MEGs [3,6–8]. Additionally, non-linear analysis methods can provide useful information about the brain dynamics in this dementia [4,5,8–10]. Nevertheless, it is desirable to develop novel strategies to help in AD detection from the analysis of the electromagnetic brain activity [9,11,12]. Techniques based on spatial filtering can help to achieve this goal, as these algorithms offer additional perspectives to examine EEG and MEG signals [11–14]. For instance, common spatial patterns (CSP) have been recently applied to enhance characteristics of EEG recordings in mild cognitive impairment (MCI) patients who eventually developed AD [11].

Another kind of spatial filtering techniques is blind source separation (BSS) [15,16]. BSS methods estimate the underlying components of the EEG and MEG signals without a priori information about those components (i.e., the components themselves and the process that produced the observed recordings are unknown) [15–17]. Since these techniques isolate specific physiological activities into different components, they have been used to reject artefacts [16–19]. This application is based on the fact that BSS isolates the artefacts into a few components. Then, the brain recordings are reconstructed without the artefactual components [18,19]. EEG and MEG data can also be processed with BSS methods to help in the recognition of neurological disorders. For example, BSS can separate specific brain activity related to epilepsy [20] or the Creutzfeldt–Jakob disease [21]. Considering these research studies, it can be hypothesised that the application of BBS, together with features extracted from electromagnetic brain activity recordings, may enhance features associated with diseases like AD. This is due to the fact that some BSS components of the EEG and MEG signals may be more sensitive to AD than others [12,14,22]. Hence, the most relevant components may be selected and the electromagnetic brain signals may be partially reconstructed using only these components to achieve a better discrimination between AD patients and healthy subjects [14].

In this work, we wanted to evaluate whether a BSS preprocessing might enhance the separation between AD patients and elderly control subjects based on spectral and non-linear features of MEG signals. Additionally, we aimed at determining whether the range of BSS components with significant differences between demented patients and controls differed when both kinds of features (spectral and non-linear ones) were considered. We also intended to confirm the results of a previous pilot study [14].

2. Subjects and magnetoencephalogram recordings

MEG recordings were acquired from 62 subjects: 36 AD patients (24 women and 12 men) and 26 elderly control subjects (17 women and 9 men). All patients were recruited from the "Asociación de Enfermos de Alzheimer" (Spain) and fulfilled the criteria of probable AD according to the guidelines of the National Institute of Neurological and Communicative Disorders and Stroke – Alzheimer's Disease and Related Disorders Association (NINCDS-ADRDA) [23]. Brain scans and thorough medical, physical, neurological, psychiatric and neurophysiological examinations were performed to diagnose the dementia. No patient was receiving medication that could affect the MEG. The control group consisted of elderly control subjects without past or present neurological disorders. Table I shows the mean and standard deviation (SD) of the age and mini-mental state examination (MMSE) score [24] for all AD patients and control subjects. It is worth noting that the difference in age between groups was not significant (p-value = 0.1911, Student's t-test). All control subjects and AD patients' caregivers gave their informed consent to participate in the study, which was approved by the local ethics committee.

INSERT TABLE 1 AROUND HERE

The population was divided randomly into a training set (18 AD patients and 13 control subjects) and a test set (formed by other 18 demented patients and 13 controls). The training set was used to develop the BSS preprocessing and to find the classification rules for each case. Then, these algorithms were applied, without further modification, to the test set to independently assess the improvement in the separation between AD patients and control subjects due to the BSS preprocessing. The demographic data and clinical features of training and test sets are also summarized in Table I.

MEG signals were acquired with a 148-channel whole-head magnetometer (MAGNES

2500 WH, 4D Neuroimaging) placed in a magnetically shielded room at the "Centro de Magnetoencefalografía Dr. Pérez-Modrego" (Spain). Five minutes of MEG were recorded from each of the subjects while they lay on a patient bed in a relaxed state, awake and with eyes closed. The sampling frequency was 678.19 Hz. To reduce data length, the recordings were decimated to 169.55 Hz. This procedure consisted of filtering the MEGs according to the Nyquist criterion and down-sampling them by a factor of four. For each subject, an average number of 17.60 ± 6.23 epochs (mean ± SD) of 10 seconds (1695 samples) that were simultaneously artefact-free at all channels were selected for analysis. Finally, signals were digitally filtered between 1.5 and 40 Hz.

3. Methods

Our methodology is introduced in the following lines. In order to test the BSS preprocessing on completely unseen data, the selection of the most sensitive components to AD was performed using the training set, whereas the assessment of the improvement in the separation between AD patients and controls was carried out with the test set. Firstly, a BSS algorithm was applied to extract the components from the MEG recordings orderly. Secondly, two spectral and two non-linear analysis methods were applied to every BSS component in the training set. For each of these four features, different ranges of components that accounted for the most significant differences between the demented patients and controls were selected to partially reconstruct the MEG signals. Afterwards, the four metrics were applied to the partially reconstructed MEG signals and to the original recordings (without the BSS preprocessing) of the training set. Subject classification rules were then derived using linear discriminant analysis (LDA). Finally, these classification thresholds for the original MEG recordings and the BSS preprocessed signals were applied to the test set in order to evaluate the enhancement in the separation between AD patients and controls due to the BSS and

component selection procedure.

3.1. Blind source separation (BSS) algorithm

BSS techniques estimate the set of n unknown components, $\mathbf{s}(t) = [s_1(t), \ldots, s_n(t)]^T$, where ^{T} denotes transposition, which were linearly mixed by the full rank $m \times n$ matrix $\mathbf{A}$ ($m \geq n$) to form m temporally and spatially correlated recordings, $\mathbf{x}(t) = [x_1(t), \ldots, x_m(t)]^T$ [15,16]. Here, $\mathbf{x}(t)$ represents the MEGs, which are related to $\mathbf{s}(t)$ by:

$$\mathbf{x}(t) = \mathbf{A}\mathbf{s}(t), \qquad (1)$$

where $\mathbf{x}(t)$ and $\mathbf{s}(t)$ are supposed to have zero mean.

Several assumptions are needed to estimate $\mathbf{s}(t)$ and $\mathbf{A}$ from $\mathbf{x}(t)$ [16,17]. The most important one is that the components are mutually independent or, alternatively, that they should be decorrelated at any time delay. Additionally, the mixing process should be linear and instantaneous. It has been proven that EEG and MEG data fulfil these hypotheses [16,17]. For simplicity, we assume that $m = n$ thanks to the fact that only the most relevant components will be retained to partially reconstruct the MEG signals. Moreover, considering $m = n$ allows us to consistently compare the same number of extracted components instead of estimating different values of n for each signal epoch [14].

Some BSS algorithms use the temporal structure of $\mathbf{x}(t)$ to compute a demixing matrix, $\mathbf{W}$. Then, the estimated inner components, $\mathbf{y}(t) = [y_1(t), \ldots, y_n(t)]^T$, are recovered by [16,18,19]:

$$\mathbf{y}(t) = \mathbf{W}\mathbf{x}(t). \qquad (2)$$

It has been shown that some BSS components may be more affected by AD than others [12,14]. Therefore, the range of the most sensitive components to AD – $\mathbf{y}_{range}(t)$ – may be back projected using the inverse of $\mathbf{W}$ ($\mathbf{W}^{-1}$) to compute a partial reconstruction of the MEGs – $\mathbf{x}_{partial}(t)$ – that may have enhanced features of AD:

$$\mathbf{x}_{partial}(t) = \mathbf{W}^{-1}\mathbf{y}_{range}(t). \quad (3)$$

Thus, features extracted from the BSS-processed signals $\mathbf{x}_{partial}(t)$ may distinguish AD patients better than those extracted from the original MEGs – $\mathbf{x}(t)$ – [12,14,22].

In contrast to other applications of BSS to EEG/MEG, we do not aim at isolating specific physiological activity [17–21]. Instead, we apply BSS as a preprocessing step to enhance the differences between AD patients and controls' brain activity [12,14,22]. Thus, $\mathbf{x}_{partial}(t)$ does not intend to resemble the brain activity accurately, but it may provide a better separation between subject groups than the MEG data without the BSS preprocessing [14].

In order to compare components from different MEG epochs and subjects and to decide which are more sensitive to AD, an order or criterion must be established [12–14]. For this reason, MEG signals were decomposed with the algorithm for multiple unknown signals extraction (AMUSE) [15,25], which provides an order for the components [12].

Considering that the components should have no correlations at any time delay, AMUSE decorrelates the input signals at two times delays, typically $\tau = 0$ and $\tau = 1$ samples [12,15,18]. This algorithm always produces the same outcome when applied to the same input dataset. Moreover, it orders the components by decreasing linear predictability [12]. Hence, it is possible to define a certain range of components – $\mathbf{y}_{range}(t)$ – by retaining only those whose index is between predefined limits. The implementation of AMUSE is as follows [12,14,25]:

1. Apply a principal component analysis to the input signals, $\mathbf{x}(t)$, to whiten them [12,25]. If $E\{\cdot\}$ denotes the expectation value of a variable, the covariance matrix of $\mathbf{x}(t)$ is computed as:

$$\mathbf{R}_x(0) = E\left\{\mathbf{x}(t)\mathbf{x}(t)^{\mathrm{T}}\right\}, \quad (4)$$

and then the whitened data, $\mathbf{z}(t)$, are estimated using [14]:

$$\mathbf{z}(t) = \mathbf{Q}\mathbf{x}(t), \quad (5)$$

where

$$\mathbf{Q} = [\mathbf{R}_x(0)]^{-1/2}. \quad (6)$$

2. Thereafter, decorrelate the signals at a particular time delay, τ (usually $\tau = 1$) [12,14,15,18]. Firstly, compute the time-delayed covariance matrix at that time delay as [25]:

$$\mathbf{R}_z(\tau) = E\left\{\mathbf{z}(t)\mathbf{z}(t-\tau)^{\mathrm{T}}\right\}, \quad (7)$$

and then compute the eigenvalue decomposition of $\left(\mathbf{R}_z(\tau) + \mathbf{R}_z(\tau)^{\mathrm{T}}\right)/2$. If $\mathbf{V}$ denotes the eigenmatrix of this decomposition, the demixing matrix $\mathbf{W}$ is calculated using [25]:

$$\mathbf{W} = \mathbf{V}^{\mathrm{T}}\mathbf{Q}\ , \quad (8)$$

and the BSS components are finally recovered with Eq. (2) [14].

3.2. Feature extraction

Every MEG channel and AMUSE component was characterised with two spectral – median frequency (*MF*) and spectral entropy (*SpecEn*) – and two non-linear features: Lempel-Ziv complexity (*LZC*) and sample entropy (*SampEn*). These features were selected on the basis of previous studies that showed their usefulness to distinguish AD patients' EEGs and MEGs from those of healthy elderly subjects [5,7,8,14,26,27]. Moreover, since two of them are spectral features (*MF* and *SpecEn*) and the other two (*LZC* and *SampEn*) are non-linear analysis methods, the usefulness of the BSS and component selection procedure could be tested with both types of techniques.

3.2.1. Median frequency (*MF*)

MF has been used to study the electromagnetic brain activity in AD [7,8] since this dementia is associated with a slowing of brain frequencies [3]. This feature summarises the signal spectrum. It provides information about the relative power of low- and high-frequency

electromagnetic oscillations produced by local synchronies of neural assemblies. In order to calculate the *MF*, the power spectral density (*PSD*) of each signal is estimated as the Fourier transform of its autocorrelation function [7]. Then, the *MF* is computed as the frequency which contains half the *PSD* power:

$$\frac{1}{2}\left[\sum_{f=1.5\text{Hz}}^{40\text{Hz}} PSD(f)\right] = \sum_{f=1.5\text{Hz}}^{MF} PSD(f). \quad (9)$$

3.2.2. Spectral entropy (*SpecEn*)

SpecEn has been applied to AD patients' EEG and MEG recordings to measure the flatness of the signal spectrum [7,26]. This is due to the fact that this dementia causes a slowing in the frequency content of the electromagnetic brain signals [3] and this measure is a convenient way of quantifying these changes. A broad and flat spectrum entails high *SpecEn* values, whereas a predictable signal with narrow spectral content offers a low *SpecEn* [28]. In order to estimate the *SpecEn*, the *PSD* is normalised (PSD_n) so that $\sum PSD_n(f) = 1$. Afterwards, *SpecEn* is computed applying the Shannon's entropy to the PSD_n [28]:

$$SpecEn = \frac{-1}{\log(N)} \sum_{f=1.5Hz}^{40Hz} PSD_n(f)\log[PSD_n(f)], \quad (10)$$

where *N* denotes the number of frequency bins and the factor $-1/\log(N)$ normalizes *SpecEn* [28].

3.2.3. Lempel-Ziv complexity (*LZC*)

LZC has been used to analyse various biomedical signals [29], including AD patients' MEG activity [27]. This metric evaluates the signal complexity by measuring the number of distinct substrings and their rate of recurrence along the time series [30]. It assigns larger values to more complex data [30]. This non-linear feature can offer information about the electromagnetic brain dynamics taking into account that it mainly depends on the signal

bandwidth and, to a smaller degree, on the sequence probability density function [29,31]. Additionally, *LZC* can be interpreted as a harmonic variability metric [29]. To compute this feature, the recording must be coarse-grained into a finite symbol sequence [29]. In this study, this transformation has been performed by comparing the data points with the median of the signal. The algorithm to compute the *LZC* can be found in [29] or [31].

3.2.4. Sample entropy (*SampEn*)

In 1991, approximate entropy was introduced to assess the irregularity of biomedical recordings by evaluating the appearance of repetitive patterns in the data [32]. This statistic counts each sequence as matching itself to avoid the occurrence of log(0) in the computations. Thus, this irregularity estimation is biased [33]. To reduce this bias, *SampEn* was developed as a modification of approximate entropy [33]. Likewise *ApEn*, *SampEn* is an irregularity metric that associates higher values with more irregular signals and it can provide information about changes in the regularity of brain local synchronizations [26]. This metric has two input parameters: a run length m and a tolerance window r [33]. In this study, *SampEn* was estimated with $m = 1$ and $r = 0.25$ times the SD of the original time series [26,33]. The implementation of the *SampEn* is detailed in [26] or [33].

3.3. Statistical analysis

Normality and homoscedasticity were verified with Kolmogorov-Smirnov and Levene's tests, respectively. Since variables met parametric test assumptions, a one-way analysis of variance (ANOVA) with age as a covariate was applied to statistically assess the differences between AD patients and control subjects' *MF*, *SpecEn*, *LZC* and *SampEn* values of the AMUSE components in the training set. The selection of the AMUSE components that were responsible for the most significant differences between the subject groups was based on the p-values obtained from this ANOVA.

The distributions of the four features before and after the BSS preprocessing were inspected visually by means of boxplots. Moreover, a linear discriminant analysis (LDA) was applied to the *MF*, *SpecEn*, *LZC* and *SampEn* values from the original MEGs (without the BSS preprocessing) and to the partially reconstructed signals of the training set. This LDA provided the optimum classification rule for the training set in each case. Then, this classification threshold was tested without further alteration on the test set. Specificity was defined as the percentage of healthy subjects correctly detected and sensitivity represented the proportion of all AD patients for whom the test was positive. Accuracy denoted the total fraction of subjects well recognised. Finally, we computed the area under the receiver-operating characteristic curve (AUC) in the test set as a summary of the separation between groups. The AUC can be interpreted as the probability that a randomly selected control subject has a value of the considered feature larger than that of a randomly chosen AD patient [34].

4. Results

4.1. Qualitative study of the AMUSE components

AMUSE was applied to blindly decompose MEG background activity epochs of 10 s (1695 samples) recorded from all 36 AD patients and 26 controls. Given that AMUSE orders the components by decreasing linear predictability [12], the *MF*, *SpecEn*, *LZC* and *SampEn* values of the components for both subject groups could be straightforwardly compared [14]. Fig. 1 depicts the values of these features for each AMUSE component averaged over all AD patients and control subjects. Overall, the values of *MF*, *SpecEn*, *LZC* and *SampEn* increased with the AMUSE component index. This relationship is particularly clear for *MF*, indicating that the order provided by AMUSE is related to the low- or high-frequency content of the components [14]. Moreover, the *SampEn* results confirm that higher AMUSE component

indexes correspond to more irregular (i.e. less predictable) data. Additionally, lower *MF*, *SpecEn*, *LZC* and *SampEn* values tended to be found in the AD patients' AMUSE components. This finding agrees with the fact that AD has been related to spectral abnormalities and a decrease in complexity and irregularity of the electromagnetic brain activity [3–5,8].

INSERT FIGURE 1 AROUND HERE

4.2. Training set results

First of all, a one-way ANOVA with age as a covariate was used to statistically assess the differences between subject groups of the training set for each AMUSE component and feature. Fig. 2 depicts these results, showing that the evolution of the *p*-values is similar for all metrics. The components with the most significant differences are gathered together and have low AMUSE components indexes, although the very first components provide less differentiation between groups. For each feature, we selected two ranges of AMUSE components that would be used to partially reconstruct the MEGs – $\mathbf{x}_{partial}(t)$. These ranges were defined as the continuous intervals of 15 and 30 components (10% and 20% of all the 148 available components, respectively) which provided the lowest average *p*-value for every metric in the training set. Table 2 shows these ranges.

INSERT FIGURE 2 AROUND HERE

INSERT TABLE 2 AROUND HERE

Afterwards, the MEG signals of the training set were partially reconstructed with the ranges specified in Table 2. An average value of *MF*, *SpecEn*, *LZC* or *SampEn* was computed per each channel and subject from these partially reconstructed signals – $\mathbf{x}_{partial}(t)$ – and from the original MEGs: $\mathbf{x}(t)$. In order to simplify the analysis, we averaged the 148 values of *MF*, *SpecEn*, *LZC* or *SampEn* for every subject [8,14]. Fig. 3 shows the corresponding boxplots computed from $\mathbf{x}(t)$ and from $\mathbf{x}_{partial}(t)$ reconstructed with 15 components in the training set. It can be observed that the BSS preprocessing modifies the distribution of the four measures, enhancing the separation between AD patients and control subjects. In order to provide additional information about the differences in the frequency content of AD patients and control subjects and how the BSS preprocessing affects the spectra, Fig. 4 depicts the average normalised Fourier spectra (PSD_n) for the original (without BSS) and the BSS preprocessed MEGs for the subjects in the training set.

INSERT FIGURE 3 AROUND HERE

INSERT FIGURE 4 AROUND HERE

Finally, LDA was applied to the average values of *MF*, *SpecEn*, *LZC* or *SampEn* of the original MEG recordings – $\mathbf{x}(t)$ – and the partially reconstructed MEG signals – $\mathbf{x}_{partial}(t)$ – to find the optimal subject classification rules in the training set. These classification rules were evaluated, without further alteration, with the test set.

4.3. Test set results

This section describes the improvement assessment in the group separation for each feature due to the BSS preprocessing. Firstly, we applied the classification rules for the case

where no component selection procedure was used – $\mathbf{x}(t)$ – to the unseen test set. The results are depicted in Table 3. Secondly, the MEGs of the test set were decomposed and the ranges of components indicated in Table 2 were used to compute partial reconstructions: $\mathbf{x}_{partial}(t)$. Then, the classification rules obtained in the training set for BSS preprocessed signals were used to classify the partially reconstructed signals of the test set. These classification results are detailed in Table 4. In addition to the accuracy, sensitivity and specificity, Tables 3 and 4 show the corresponding AUCs computed in each case for the test set. It can be seen that, except for the *MF*, the component selection procedure provided increases in the accuracy between 6.4% and 22.6% in comparison with the case where no BSS preprocessing was used. Additionally, the improvement in the AUC due to the BSS preprocessing ranged between 0.013 and 0.227.

INSERT TABLE 3 AROUND HERE

INSERT TABLE 4 AROUND HERE

---

5. Discussion and conclusions

AMUSE was applied to decompose artefact-free MEG epochs of 36 AD patients and 26 controls. The population was divided randomly into training and test sets to avoid the optimization of the parameters involved in the methodology (ranges of components and classification rules) on the whole dataset. Every component was characterised with two spectral (*MF* and *SpecEn*) and two non-linear (*LZC* and *SampEn*) features. For each of these metrics, a one-way ANOVA with age as a covariate was used to decide which components had the most significant differences between AD patients and controls in the training set.

These ranges of components were used to compute the partial reconstructions of the MEG signals: $\mathbf{x}_{partial}(t)$. LDA provided the classification rules for each case in the training set. Then, these rules were applied to the test set without further modification to compare the separation between groups achieved using the original MEG recordings and with that of the partially reconstructed MEGs. The results suggest that the BSS and component selection procedure improves the separation between the AD patients and control groups since this preprocessing usually increased both the accuracy and AUC.

The BSS and component selection procedure increased the accuracy between 6.4% and 22.6% for all features apart from *MF*, for which the accuracy remained unchanged or decreased (-6.4%) when the BSS preprocessing was applied. Nevertheless, the AUCs of all features improved between 0.013 and 0.227. It is remarkable that our accuracy and AUC results were computed in different ways. Whereas the accuracy was calculated in the test set with the classification rules developed in the training set, the AUC was estimated using data only from the test set. Furthermore, in contrast to the maximum accuracy value obtained for a variable, the AUC depends on the whole range of sensitivity/specificity pairs provided by that variable, thus offering an idea of how separated the groups are [34]. Therefore, our results suggest that the BSS preprocessing provide a more robust separation between groups for both kinds of features: spectral and non-linear ones. Moreover, our analyses showed that similar ranges of components contained the most significant differences for both types of features. These ranges only differ slightly in the case of *MF*. Therefore, it could be hypothesised that this BSS and component selection procedure could also be applied with other spectral and non-linear features and that the ranges of components with the largest differences between AD patients and healthy controls for other analysis techniques might be similar to those reported in this study.

Previous research by other authors had shown the utility of the BSS and component selection preprocessing when spectral and time-scale features were computed from EEGs of MCI patients who later proceeded to AD [12,22]. These EEG signals were characterised with the relative powers in six frequency bands [12]. Afterwards, an LDA was applied to classify the subjects. The accuracy improvement due to this methodology was 10% [12]. Nevertheless, the individual improvement in each variable was not measured in [12]. Additionally, a later study used a "bump modelling" of the partially reconstructed EEG wavelet time-frequency transform and a neural network classifier to further improve the subject classification [22]. In contrast to these studies, our classification method allowed us to assess the improvement in each variable (*MF*, *SpecEn*, *LZC* or *SampEn*) separately. We have also found that the BSS and component selection procedure is useful when the MEG signals are analysed with non-linear methods. Similarly, a study with the same EEGs analysed in [12] and [22] found that the ability of both spectral and non-linear features to distinguish the subject groups improved with the application of a different kind of spatial filters: CSP [11]. CSP finds spatial filters which maximise the difference in signal power between two classes to be discriminated (e.g., patients and controls) [11]. Since different spatial filtering techniques have proven to be useful in this application, it is necessary to test other algorithms which may also provide improvements in the classification of healthy elderly subjects and patients with neurological disorders.

Certain limitations of our study merit consideration. First of all, the sample size was small. Although the AD patients and control subjects were divided randomly into a training set and a test set to evaluate the methodology with completely unseen data, our results should be taken with caution. Additional analysis with a larger database should be performed. A training set with a higher number of subjects would allow us to develop a more consistent and optimised preprocessing methodology, while a larger test set would increase the reliability of

the estimated results. Moreover, it could be particularly interesting to distinguish MCI patients from control subjects in order to predict AD [12]. Additionally, given the fact that this application of spatial filtering techniques is relatively new, the performance of other algorithms should be tested.

To sum up, this paper describes a BSS and component selection preprocessing to improve the separation between spectral and non-linear features extracted from AD patients and control subjects' MEG activity. In order to avoid the optimization of the parameters involved in the BSS preprocessing on the whole population, the subjects were divided randomly into training and test sets. Thanks to the fact that the BSS algorithm (AMUSE) orders the extracted components by decreasing linear predictability [12], it was possible to compare components extracted from AD patients and control subjects to decide which of them provided more significant group differences in the training set. Then, these significant components were projected back to the MEG signals, and these partially reconstructed MEGs were characterised with spectral and non-linear features. The improvement in the group separation was compared with the case where no BSS preprocessing was applied to the same MEG recordings in the test set. This preprocessing increased the AUC for all features between 0.013 and 0.227 while the accuracy rose in three of the four features between 6.4% and 22.6%. These results suggest that the BSS and component selection procedure improves the group separation, thus corroborating previous studies [14].

Acknowledgements

This work has been supported in part by the “Ministerio de Educación y Ciencia” and FEDER grant MTM 2005-08519-C02-01 and by the grant project VA108A06 from “Consejería de Educación de Castilla y León”. J. Escudero was in receipt of an FPU grant from the Spanish Government. The authors are thankful to the Referees for their useful

comments on the original version of the manuscript and to the “Asociación de Familiares de Enfermos de Alzheimer” (Spain) for supplying the patients who took part in this study.

References

[1] Hari R. Magnetoencephalography in clinical neurophysiological assessment of human cortical functions. In: Niedermeyer E, Lopes da Silva F, editors. 'Electroencephalography: basic principles, clinical applications, and related fields'. Philadelphia: Lippincontt Williams & Wilkins, 2005:1165–97.

[2] Blennow K, de Leon MJ, Zetterberg H. Alzheimer's disease. Lancet 2006;368:387–403.

[3] Jeong J. EEG dynamics in patients with Alzheimer's disease. Clin Neurophysiol 2004;115:1490–505.

[4] Stam CJ. Nonlinear dynamical analysis of EEG and MEG: Review of an emerging field. Clin Neurophysiol 2005;116:2266–301.

[5] Hornero R, Abásolo D, Escudero J, Gómez C. Nonlinear analysis of electroencephalogram and magnetoencephalogram recordings in patients with Alzheimer's disease. Phil Trans R Soc A 2009;367:317–36.

[6] Signorino M, Pucci E, Belardinelli N, Nolfe G, Angeleri F. EEG spectral analysis in vascular and Alzheimer dementia. Electroencephalogr Clin Neurophysiol 1995;94:313–25.

[7] Poza J, Hornero R, Abásolo D, Fernández A, García M. Extraction of spectral based measures from MEG background oscillations in Alzheimer's disease. Med Eng Phys 2007;29:1073–83.

[8] Hornero R, Escudero J, Fernández A, Poza J, Gómez C. Spectral and non-linear analyses of MEG background activity in patients with Alzheimer's disease. IEEE Trans Biomed Eng 2008;55:1658–65.

[9] Henderson G, Ifeachor E, Hudson N, Goh C, Outram N, Wimalaratna S, Del Percio C, Vecchio F. Development and assessment of methods for detecting dementia using the human electroencephalogram. IEEE Trans Biomed Eng 2006;53:1557–68.

[10] Park J-H, Kim S, Kim C-H, Cichocki A, Kim K. Multiscale entropy analysis of EEG from patients under different pathological conditions. Fractals-Complex Geom Patterns Scaling Nat Soc 2007;15:399–404.

[11] Woon WL, Cichocki A, Vialatte F, Musha T. Techniques for early detection of Alzheimer's disease using spontaneous EEG recordings. Physiol Meas 2007;28:335–47.

[12] Cichocki A, Shishkin SL, Musha T, Leonowicz Z, Asada T, Karachi T. EEG filtering based on blind source separation (BSS) for early detection of Alzheimer's disease. Clin Neurophysiol 2005;116:729–37.

[13] Jin SH, Jeong J, Jeong DG, Kim DJ, Kim SY. Nonlinear dynamics of the EEG separated by independent component analysis after sound and light stimulation. Biol Cybern 2002;86:395–401.

[14] Escudero J, Hornero R, Poza J, Abásolo D, Fernández A. Assessment of classification improvement in patients with Alzheimer's disease based on magnetoencephalogram blind source separation. Artif Intell Med 2008;43:75–85.

[15] Cichocki A, Amari S. 'Adaptive blind signal and image processing: learning algorithms and applications.' John Wiley & Sons, Ltd. Cichester, West Sussex, England, 2003.

[16] James CJ, Hesse CW. Independent component analysis for biomedical signals. Physiol Meas 2005;26:R15–39.

[17] Vigário R, Oja E. Independence: a new criterion for the analysis of the electromagnetic fields in the global brain? Neural Netw 2000;13:891–907.

[18] Ting KH, Fung PCW, Chang CQ, Chan FHY. Automatic correction of artefact form single-trial event-related potentials by blind source separation using second order statistics only. Med Eng Phys 2006;28:780–94.

[19] Escudero J, Hornero R, Abásolo D, Fernández A, López-Coronado M. Artifact removal in magnetoencephalogram background activity with independent component analysis. IEEE Trans Biomed Eng 2007;54:1965–73.

[20] Kobayashi K, James CJ, Nakatori T, Akiyama T, Gotman J. Isolation of epileptiform discharges from unaveraged EEG by independent component analysis. Clin Neurophysiol 1999;110:1755–63.

[21] Hung C-I, Wang P-S, Soong B-W, Teng S, Hsieh J-C, Wu Y-T. Blind source separation of concurrent disease-related patterns from EEG in Creutzfeldt–Jakob disease for assisting early diagnosis. Ann Biomed Eng 2007;35:2168–79.

[22] Vialatte F, Cichocki A, Dreyfus G, Musha T, Gervais R. Early detection of Alzheimer's disease by blind source separation and bump modelling of EEG signals. Lect Notes Comput Science 2005;3696:683–92.

[23] McKhann G, Drachman D, Folstein M, Katzman R, Price D, Stadlan EM. Clinical diagnosis of Alzheimer's disease: report of the NINCDS-ADRDA Work Group under the auspices of Department of Health and Human Services Task Force on Alzheimer's disease. Neurology 1984;34:939–44.

[24] Folstein MF, Folstein SE, McHugh PR. Mini-mental state. A practical method for grading the cognitive state of patients for the clinician. J Psychiatr Res 1975;12:189–98.

[25] Tong L, Liu R, Soon VC, Huang Y-F. Indeterminacy and identifiability of blind identification. IEEE Trans Circuits Syst 1991;38:499–509.

[26] Abásolo D, Hornero R, Espino P, Álvarez D, Poza J. Entropy analysis of the EEG background activity in Alzheimer's disease patients. Physiol Meas 2006;27:241–53.

[27] Gómez C, Hornero R, Abásolo D, Fernández A, López M. Complexity analysis of the magnetoencephalogram background activity in Alzheimer's disease patients. Med Eng Phys 2006;28:851–9.

[28] Sleigh JW, Steyn-Ross DA, Grant C, Ludbrook G. Cortical entropy changes with general anaesthesia: theory and experiment. Physiol Meas 2004;25:921–34.

[29] Aboy M, Hornero R, Abásolo D, Álvarez D. Interpretation of the Lempel-Ziv complexity measure in the context of biomedical signal analysis. IEEE Trans Biomed Eng 2006;53:2282–8.

[30] Lempel A, Ziv J. On the complexity of finite sequences. IEEE Trans Inf Theory 1976;IT-22:75–81.

[31] Ferenets R, Lipping T, Anier A, Jäntti V, Melto S, Hovilehto S. Comparison of entropy and complexity measures for the assessment of depth of sedation. IEEE Trans Biomed Eng 2006;53:1067–77.

[32] Pincus SM. Approximate entropy as a measure of system complexity. Proc Natl Acad Sci USA 1991;88:2297–301.

[33] Richman JS, Moorman JR. Physiological time-series analysis using approximate entropy and sample entropy. Am J Physiol (Heart Circ Physiol) 2000;274: H2039–49.

[34] Zweig MH, Campbell G. Receiver-Operating Characteristic (ROC) plots: a fundamental evaluation tool in clinical medicine. Clin Chem 1993;39:561–77.

Table legends

Table 1. Demographic and clinical features for all participants, and the training and test sets. Data are given as mean ± SD.

All subjects		
	AD patients	Control subjects
Number of subjects	36	26
Number of females	24	17
Age (years)	74.06 ± 6.95	71.77 ± 6.38
MMSE score	18.06 ± 3.36	28.88 ± 1.18
Training set		
	AD patients	Control subjects
Number of subjects	18	13
Number of females	12	9
Age (years)	74.11 ± 7.38	71.38 ± 4.84
MMSE score	17.72 ± 3.63	28.92 ± 1.04
Test set		
	AD patients	Control subjects
Number of subjects	18	13
Number of females	12	8
Age (years)	74.00 ± 6.70	72.15 ± 7.82
MMSE score	18.39 ± 3.15	28.85 ± 1.34

Table 2. Ranges of AMUSE components (estimated from the training set) selected to partially reconstruct the MEG signals for each feature.

Retained components	*MF*	*SpecEn*	*LZC*	*SampEn*
Subset of 15 components (10%)	18 to 32	9 to 23	7 to 21	7 to 21
Subset of 30 components (20%)	13 to 42	6 to 35	3 to 32	6 to 35

Table 3. Classification results and AUC obtained from the MEG recordings without the BSS preprocessing in the test set using the decision rules developed with the training set.

	MF	*SpecEn*	*LZC*	*SampEn*
Accuracy (%)	77.4	61.3	61.3	58.1
Sensitivity (%)	88.9	55.6	55.6	72.2
Specificity (%)	53.9	69.2	69.2	38.5
AUC	0.855	0.727	0.786	0.645

Table 4. Classification results and AUC obtained from the partially reconstructed MEG signals in the test set using the algorithms developed with the training set.

	MF		*SpecEn*		*LZC*		*SampEn*	
Number of components retained	30 (20%)	15 (10%)	30 (20%)	15 (10%)	30 (20%)	15 (10%)	30 (20%)	15 (10%)
Accuracy (%)	77.4	71.0	71.0	67.7	67.7	74.2	80.7	80.7
Sensitivity (%)	77.8	66.7	77.8	72.2	72.2	72.2	83.3	83.3
Specificity (%)	76.9	76.9	61.5	61.5	61.5	76.9	76.9	76.9
AUC	0.878	0.868	0.786	0.782	0.838	0.838	0.872	0.863

Figure legends

Fig. 1. Average values of (a) *MF*, (b) *SpecEn*, (c) *LZC* and (d) *SampEn* for every AMUSE component in all AD patients and control subjects.

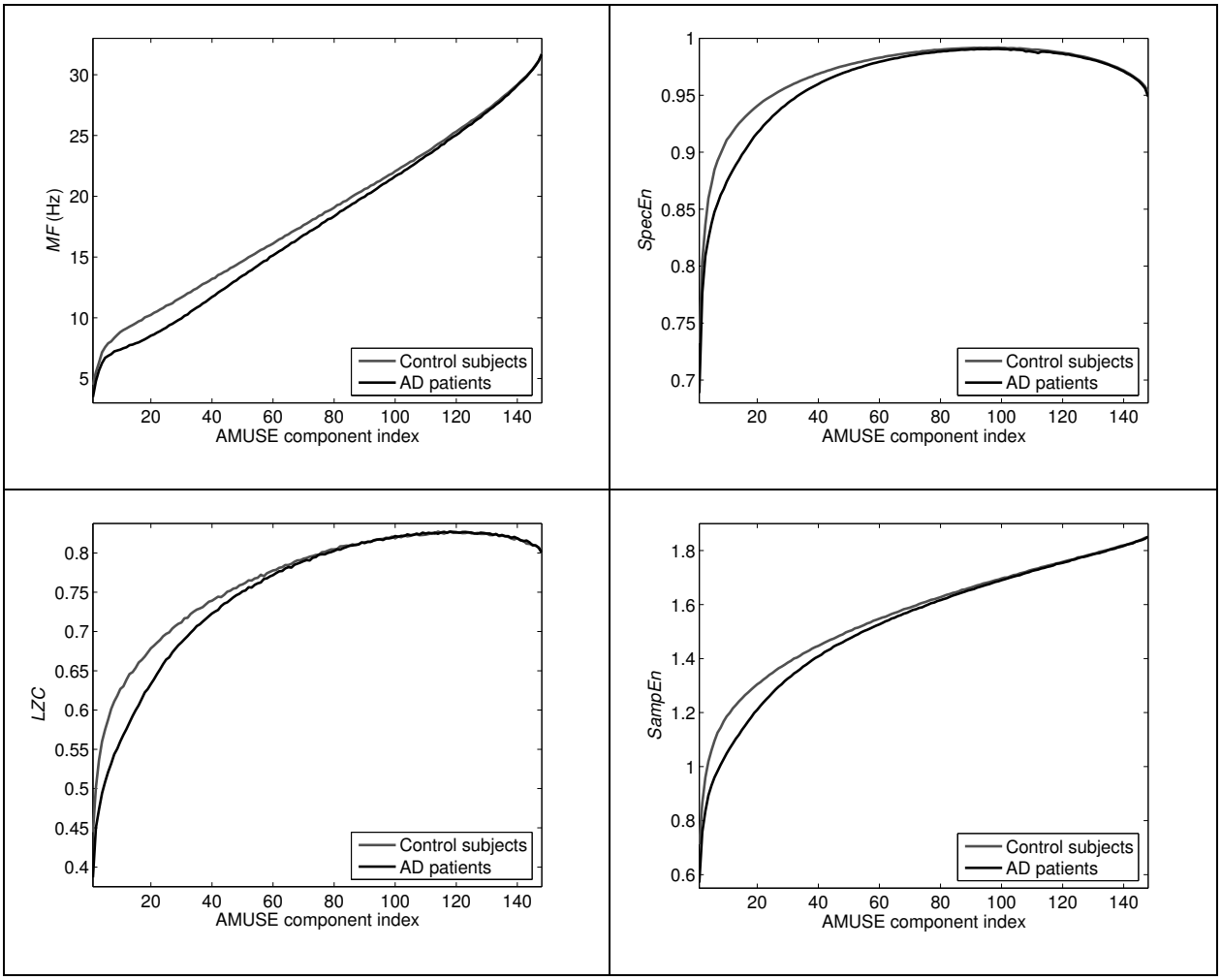

Fig. 2. *p*-values of a one-way ANOVA with age as a covariate computed for each AMUSE component in the training set for (a) *MF* and *SpecEn* and (b) *LZC* and *SampEn*.

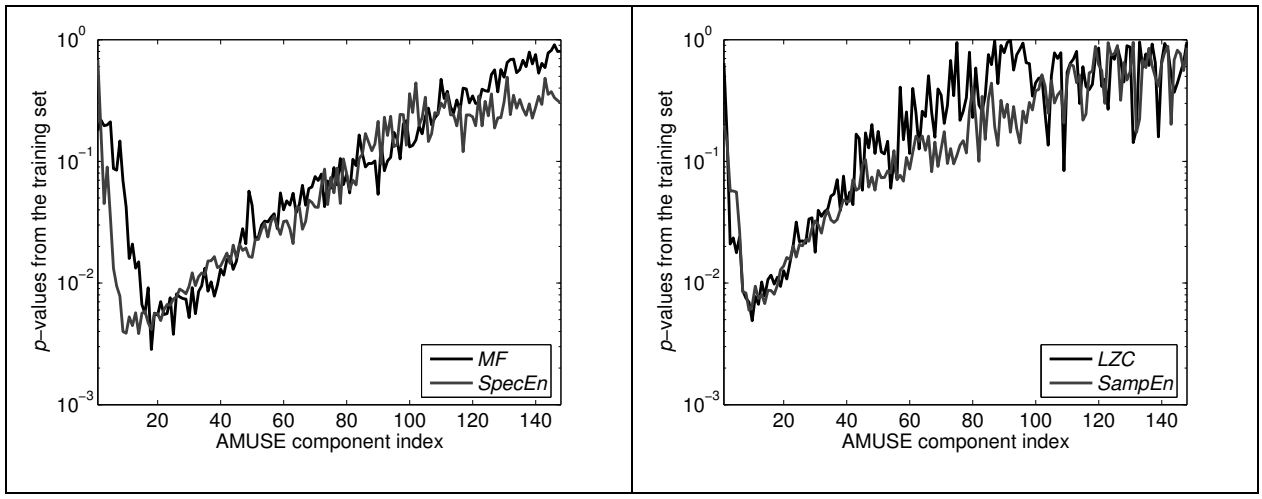

Fig. 3. Boxplots for (a) *MF*, (b) *SpecEn*, (c) *LZC* and (d) *SampEn* computed using the original MEG recordings without the BSS preprocessing and the MEGs partially reconstructed with 15 components from AD patients (AD) and control subjects (CS) in the training set.

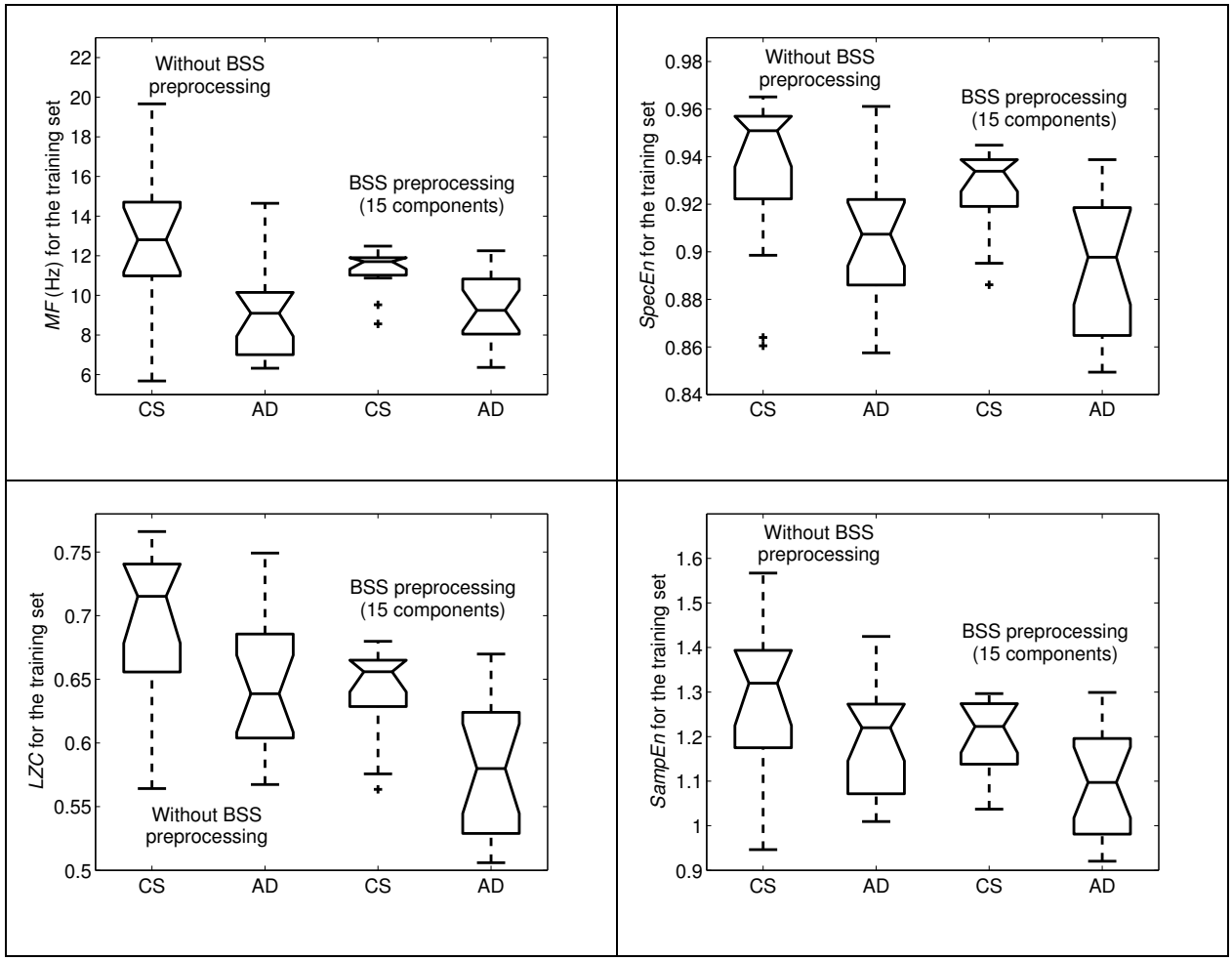

Fig. 4. Normalised frequency spectra (PSD_n) for AD patients and control subjects in the training set computed using (a) the original MEG recordings without the BSS preprocessing and (b) the MEGs partially reconstructed with components 9 to 23.